

RESEARCH ARTICLE

Terpolymer-chitosan membranes as biomaterial

María Leticia Bravi Costantino^{1,2} | María Soledad Belluzo¹ | Tamara G. Oberti¹  | Ana M. Cortizo² | María Susana Cortizo¹

¹Instituto de Investigaciones Físicoquímicas Teóricas y Aplicadas (INIFTA), Facultad de Ciencias Exactas, UNLP–CONICET, La Plata, Argentina

²Laboratorio de Investigaciones en Osteopatías y Metabolismo Mineral (LIOMM), Facultad de Ciencias Exactas, UNLP–CIC, La Plata, Argentina

Correspondence

Tamara G. Oberti, CC 16, Suc 4, La Plata, Argentina.

Email: toberti@inifta.unlp.edu.ar

Funding information

Consejo Nacional de Investigaciones Científicas y Técnicas, Grant/Award Number: PIP D0047; Universidad Nacional de La Plata, Facultad de Ciencias Exactas, Grant/Award Number: 11/X769; CONICET, Grant/Award Number: PIP D0047; Universidad Nacional de La Plata, Grant/Award Number: 11/X769

Abstract

The present study shows a novel copolymer synthesis, its application in the membrane design and the physicochemical and biological characterization of the biomaterial obtained. Terpolymer starting diisopropyl fumarate (F), vinyl benzoate (V) and 2-hydroxyethyl methacrylate (H) was prepared by thermal radical polymerization. This polymer (FVH) was obtained in several monomer ratios and characterized by spectroscopic and chromatographic methods (FTIR, ¹H-NMR and SEC). The best relationship of F:V:H was 5:4:1, which allows efficient interaction with chitosan through cross-linking with borax to achieve scaffolds for potential biomedical applications. The membranes were obtained by solvent casting and analyzed by scanning electron microscopy (SEM), swelling behavior and mechanical properties. In addition, we studied the possible cytotoxicity and biocompatibility of these materials using a murine macrophage-like cell line (RAW 264.7) and bone marrow mesenchymal progenitor cells (BMPC), respectively, taking into account their intended applications. The results of this study show that the terpolymer obtained and its combination with a natural polymer is a very interesting strategy to obtain a biomaterial with possible applications in regenerative medicine and this could be extended to other structurally related systems.

KEYWORDS

biomaterials, chitosan, cytotoxicity, fumaric polymers, swelling

1 | INTRODUCTION

According to the European Society for Biomaterials Consensus Conference-II, a biomaterial is defined as the material anticipated interfacing in our biological systems in order to estimate the augment, treat or replacement of any tissue, organ or the functioning of the body.¹ In tissue engineering, the use of biomaterials has been investigated for some years in different types of tissue: bone^{2,3}; skin,⁴ articular cartilage,⁵ etc. Biomaterials employed in tissue regeneration have been developed using different types of natural or synthetic polymers, such as alginate, gelatin, dextran, chitosan, cellulose^{6,7} or acrylates and methacrylate polyesters, among others.⁸

In our study group, various fumaric homo and copolymers have been synthesized and studied since they are derived from fumaric

esters, which can be easily obtained from maleic anhydride, a by-product of the oil industry. Fumaric polymers can be considered competitive with methacrylics polymers because they exhibit similar physicochemical properties.^{9,10} Poly (diisopropyl fumarate) homopolymer (PDIPF) has been shown to be a material with high thermal stability but fragile. However, the mechanical properties can be modified by mixture with other polymers or by copolymerization with other comonomers.^{11,12} Likewise, we have shown that the combination of synthetic and natural polymers constitutes a versatile and efficient alternative to develop novel materials with varied properties that cannot be achieved through the use of individual polymers.^{13,14}

On other hand, one of the most used biopolymers is chitosan (Ch), which is obtained by deacetylation of chitin. Chitin is a polysaccharide component of the exoskeleton of arthropods such as lobster

and crab, or the endoskeleton of cephalopod mollusks such as squid, which represent common waste materials from the fishing industry.¹⁵ Derivative Ch is a linear polysaccharide composed of randomly distributed units of glucosamine and N-acetylglucosamine linked by β -(1,4)-glycosidic bonds, and the relationship between these subunits determines the degree of acetylation of chitosan, which influences in many of its properties. Its main characteristics are: low toxicity, non-immunogenicity, biodegradability, biocompatibility, ability to form films, and easy accessibility.¹⁶ The presence of the proton-acceptor amino group along the glucosamine residues allows us to understand most of the properties of Ch.¹⁷ Added to this, its cationic nature allows it to interact with negatively charged polymers and structural molecules present in the extracellular matrix of various tissues of the human body.¹⁸ However, its weak mechanical properties and very rapid biodegradation make chitosan by itself not useful for regeneration of bone tissue. In order to overcome these drawbacks, some researchers have proposed its combination with different synthetic polymers, such as poly (vinyl alcohol), poly(ϵ -caprolactone), and others.¹⁹⁻²¹

Based on the previous information, a new terpolymer was synthesized starting with diisopropylfumarate (DIPF), vinyl benzoate (VBz) and 2-hydroxyethyl methacrylate (HEMA). In order to replace the acrylic monomers, a fumaric monomer was selected and thus obtain cheaper materials. The VBz was selected based on copolymerization behavior between fumaric esters with vinyl monomer carrying electron donating substituent.^{9,22} The third comonomer, HEMA, provides the hydroxyl groups that will interact with the crosslinking agent.²³ Then, in order to obtain a material with appropriate characteristics for the intended application, a membrane was designed making the synthetic copolymer compatible with chitosan, through the hydroxyl functional groups which can be cross-linked by borax as a cross-linking agent. Finally, the biomaterial was physicochemical characterized and its biocompatibility and possible cytotoxicity were evaluated.

2 | EXPERIMENTAL SECTION

2.1 | Materials

Diisopropyl fumarate (DIPF) monomer was prepared and purified in our laboratory as previously described.²⁴ Briefly, fumaric acid (Biopack, Pure) and isopropanol (Sintorgan) were added to toluene (Cicarelli), in 1:2.65 ratio, with a catalytic amount of sulfuric acid (Merck, 95–97%) and the mixture was refluxed for 22 h. The product was purified by distillation under vacuum (yield 76%). Vinyl benzoate (VBz) was purchased from Aldrich and distilled before use. 2-Hydroxyethyl methacrylate (HEMA), was purchased from Sigma-Aldrich and was purified by filtration through neutral alumina prior to use. 2,2-Azobisisobutyronitrile (AIBN) were purchased from MERCK (Buenos Aires, Argentina) and used after recrystallization from methanol. Borax, from Timper Laboratorios (99.9%) was used as received without further purification. Chitosan (Ch, low molecular weight) was purchased from Sigma-Aldrich. Toluene, Hexane, Chloroform, and

other solvents with analytical grade, were purchased from Anedra (Buenos Aires, Argentina).

2.2 | Copolymer synthesis

For the copolymer synthesis, different molar relations of the monomers (see Table 1) were tested in order to obtain a copolymer capable of effectively interact with the hydroxyl groups of the chitosan to form the scaffolds. In all cases, thermal radical copolymerization of diisopropyl fumarate (F), vinyl benzoate (V) and 2-hydroxyethyl methacrylate (H) was carried out in THF solution under thermal heating at 60°C. Briefly, copolymerization was carried out introducing all the monomers and the solvent into a reaction tube with a pre-weighed amount of initiator (AIBN, 15 mM). The mixtures were degassed by three freeze-pump-thaw cycles in a vacuum line system, then they were heated, sealed and immersed into a thermostat at 60°C with stirring. After a certain time (14–28 h), the terpolymer (FVH) was isolated by dissolution in THF and purified by precipitation in water-methanol (90:10). Finally, the polymers were dried at constant weight for conversion (%C) estimation by gravimetry.

2.3 | Copolymer characterization

The terpolymers were characterized by several techniques. ¹H-NMR spectra of polymers were recorded with a Bruker Avance NEO 500 spectrometer at 35°C in Acetone-D₆. Tetramethylsilane (TMS) was used as an internal standard. This technique was performed to determine the copolymers composition as it will be detailed in the results section. Fourier transform infrared spectra (FTIR) were carried out on a Shimadzu FTIR (IR affinity-S1) between 4000 to 400 cm⁻¹ with a resolution of 4 cm⁻¹ and 40 accumulated scans. The EZ-OMNIC software (Thermo Fisher Scientific Inc.) was used to analyze the spectra. The molecular weight distribution and the average molecular weights were determined by size exclusion chromatography (SEC), using a LKB-2249 instrument at 25°C. A series of four μ -Styragel columns, ranging in pore size 10⁵, 10⁴, 10³, 100 Å, were used with chloroform as eluent. The sample concentration was 15 mg/ml and the flow rate was 0.5 ml/min. The polymer was detected by infrared (Miram 1A Infrared Analyzer) and UV (Shimadzu UV-VIS SPD-10A, 254 nm) detection using trichlorobenzene (TCB) as internal standard. The calibration was done with polystyrene standards.

2.4 | Membranes preparation

The scaffolds were prepared through the solvent-casting method. In this case, a 1%w/v chitosan solution in a 3%v/v acetic acid was prepared. Then, the previous solution was mixed with 2%w/v FVH solution in glacial acetic acid with a 1:3 ratio (Ch/FVH). The procedure was adapted from a previous study from our group.¹⁴ Briefly, the chitosan solution was added dropwise into a FVH solution with

stirring in a thermostated water bath at 60°C. When Ch dropped was complete, borax (4%w/w of the mixture of Ch/FVH, previously dissolved in water) was added to cross-link the polymers. Finally, the mixture was placed in Teflon molds and dried by solvent evaporation at 25°C. The obtained membranes were dried under vacuum until constant weight. In all cases, membranes were neutralized prior to use with NaOH (5%w/v) in order to achieve a neutral pH, essential for biological tests. As part of the characterization, a physical mixture between FVH and Ch was prepared, by mixing the polymers (without the borax addition) and evaporating the solvent at room temperature. The membranes were designated Ch-FVH-B and Ch-FVH, with and without borax addition, respectively.

2.5 | Membranes characterization

2.5.1 | SEM analysis

The membranes, both surfaces and cross section (obtained by freeze fracture in liquid nitrogen), were coated with gold and their morphology was examined during scanning electron microscopy (SEM, Philips 505) with an accelerating voltage of 20 kV. The images for macroscopic observation were taken with a Nikon D3400 camera.

The thickness of the membranes was measured using a micrometer (Black Jack, 0–25 mm ± 0.01) and mean values were determined.

2.5.2 | Differential scanning calorimetry analysis

Glass transition temperature (T_g) of Ch-FVH and Ch-FVH-B membranes was determined by differential scanning calorimetry (DSC, Q2000-TA Instruments). The samples were scanned at 10°C/min, from –20 to 150°C, under dry nitrogen. Three consecutive scans were performed for each sample: heating/cooling/heating. For comparison T_g of Ch and FVH were also determined.

2.5.3 | Swelling test

The maximum swelling and water absorption capacity of the membranes were determined as described before.¹² The previously weighted samples were placed in a suitable vessel and incubated at 37°C. Buffer Phosphate (PBS, pH 7.4) was used as media. The temperature and medium of this test were selected taking into account that the designed materials could be used in biological application. After incubation, the exceeding solution was removed with filter paper and the samples were weighed. The maximum swelling percentage of the membranes was defined as shown in Equation (1). Water content of the membrane was obtained as the difference between the weights of the water saturated sample (w) and the weight of the initial dried sample (w_0):

$$\%S_w = \frac{100(w - w_0)}{w_0} \quad (1)$$

For each time, the % Sw values presented are the mean values of four independent measurements.

In order to analyze the swelling mechanism, that is, the water transport process through the membrane, the Ritger-Peppas model was used,²⁵ according to the following equation:

$$\frac{W_t}{W_\infty} = k t^n \quad (2)$$

where k is a characteristic constant of the system, which depends on the structural characteristics of the polymer and its interaction with the solvent, n is the swelling exponent, which describes the mechanism of water transport into the membrane, while w_t and w_∞ represent the quantities of water absorbed at time t and at equilibrium time, respectively. In Equation (2), the numerical n value provides information about the water sorption mechanism. An n value close to 0.50 indicates a transport mechanism controlled by Fick diffusion or case I (water diffusion rate is lower than the relaxation rate of polymer chains). When $n = 1$, the transport mechanism is controlled by a diffusion case II (the water diffusion is higher than relaxation processes). However, a value of n between 0.50 and 1.00 implies that the transport mechanism exhibits a non-Fickian diffusion process in which the relaxation of polymer chains determines the rate of water sorption.^{26,27} The value of n can be obtained from the slope, while k is obtained from the interception of the $\log(w_t/w_\infty)$ plot versus $\log t$ from the experimental data, taken until 60% of the maximum swelling.

2.6 | Mechanical Testing

The tensile properties of the biomaterial were determined using a universal testing machine (Digimes TC500) with 50 N capacity force load cell, following the methodology previously described.²⁸ The samples were linear stripes of 35 cm long, 13 mm wide, and a thickness of 0.28 mm. They were placed in a controlled humidity media (70%) overnight, previously to perform the test. The elastic modulus, tensile strength and elongation at break were determined from the slope in the linear region of the curve. The results presented are the mean values of seven independent measurements.

2.7 | Biocompatibility and cytotoxicity studies

2.7.1 | Cell culture and incubation

For the *in vitro* experiment we used bone marrow mesenchymal progenitor cells (BMPC) and murine macrophage RAW 264.7. The latter cell line acts as a model to emulate the inflammatory response “*in vitro*” and it has been previously used in our laboratory to evaluate the possible cytotoxicity of different biomaterials.^{29,30}

Murine macrophage RAW 264.7 cells were grown in DMEM (Invitrogen, Buenos Aires, Argentina) supplemented with 10%v/v fetal bovine serum (FBS, Natacor, Argentina) and antibiotics (100 UI/ml

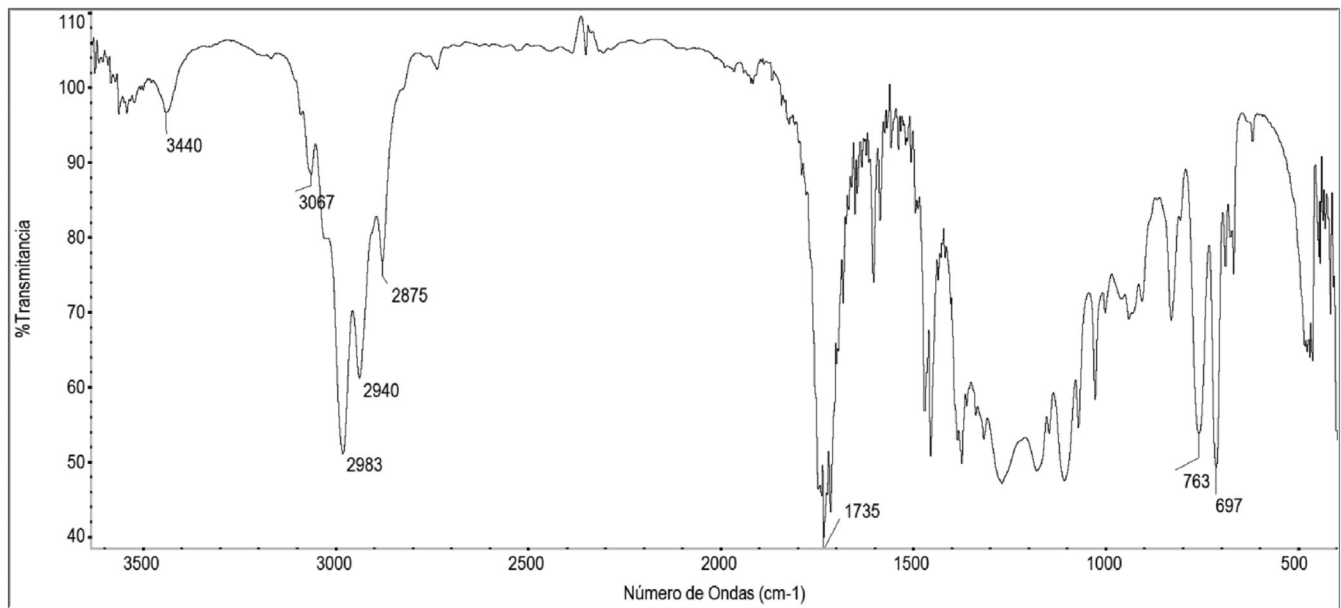


FIGURE 1 FTIR spectrum of FVH-4

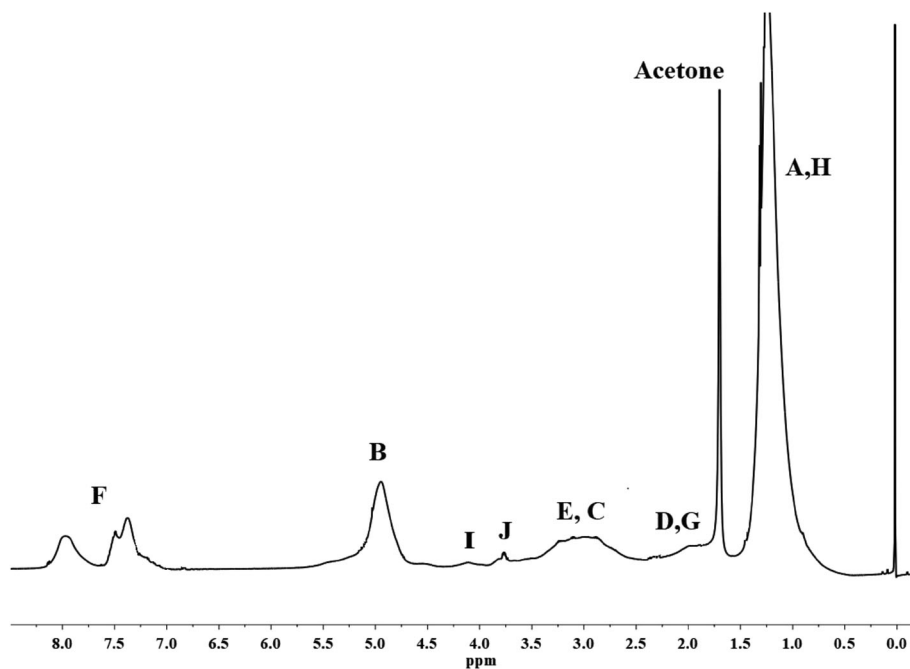


FIGURE 2 ^1H -NMR spectrum of FVH-4

penicillin and 100 mg/ml streptomycin) at 37°C in a 5% CO_2 atmosphere. BMPC were isolated from the femora of Sprague–Dawley rats and cultured according to standard procedures used in our laboratory.^{29,30} Cells were maintained in basal media (DMEM-10% FBS) at 37°C. For all the experiments, circular samples of 8 mm in diameter and 2 mm in thickness were used. All experiments to isolate cells from animals were performed in conformity with the Guidelines on Handling and Training of Laboratory Animals, published by the Universities Federation for Animals Welfare. Approval for animal studies was

obtained from our institutional animal welfare committee (CICUAL-FEC-UNLP Protocol Number 001-05-15).³¹

2.7.2 | Cell viability

Cell viability was tested using 3-(4,5-dimethylthiazol-2-yl)-2,5-diphenyl tetrazolium bromide (MTT) assay.¹⁴ The membranes were inserted in a 24-well plate, sterilized by irradiation with UV light for

20 min. The samples were washed with DMEM and seeded with RAW 264.7 macrophages in 1% FBS-DMEM. After 2 h of incubation time in a humidified atmosphere of 95% air and 5% CO₂ (adhesion), the conditioned medium of RAW 264.7 cells was aspirated and replaced by a medium without phenol red, supplemented with 1% FBS and incubated for 24 h (proliferation). After this period, cells were incubated for 2 additional hours with 0.1 mg/ml MTT solution. After washing, 200 µl of dimethyl sulfoxide (DMSO) were added and the absorbance was read at 570 nm using an ELISA reader (Infinite F50, tecan trading AG, Switzerland).

The morphology of RAW 264.7 cells seeded on the membranes was evaluated by SEM images after 24 h of cell culture. After the incubation period, samples were washed with PBS, fixed with 10% paraformaldehyde (10 min at room temperature), dehydrated with methanol (5 min) and dried. Finally, the samples were coated with gold and SEM images were obtained (SEM, Philips 505).

The BMPC viability was determined using MTT assay, after 2 and 48 h of cell culture on the scaffolds under similar conditions as previously described.³⁰

2.7.3 | Cytotoxicity evaluation

The possible cytotoxicity of the biomaterials was evaluated by Nitric oxide (NO) production into the culture media after 24 h. NO production was assessed in the culture media by Griess' reaction,³² using RAW 264.7 cells. Briefly, 500 µl samples of conditioned media and nitrite standards 0–100 nM were mixed with 500 µl of Griess' reagent (1% sulfanilamide and 0.1% naphthylethylene-diamine in 5% phosphoric acid) and absorbance was measured at 550 nm against a blank prepared with non-conditioned medium. RAW 264.7 cells were also plated on standard culture tissue dishes with lipopolysaccharide (LPS, 0.1 µg/ml) as positive controls.⁶

2.7.4 | Statistical analysis

Results are expressed as mean ± SE and, unless indicated otherwise, were obtained from at least three different experiments performed in triplicate. Differences between the groups were assessed by one-way analysis of variance (ANOVA) using the Tukey post hoc test. For no normally distributed data, the nonparametric Kruskal–Wallis test with

the Dunn post hoc test was performed using GraphPad In Stat version 3.00 (Graph Pad Software, San Diego, California). $p < .05$ was considered significant for all statistical analyses.

3 | RESULTS

3.1 | Copolymer synthesis and characterization

Copolymers of diisopropyl fumarate (F), vinyl benzoate (V) and 2-hydroxyethyl methacrylate (H), designated as FVH, were synthesized by conventional radical polymerization. Table 1 summarizes characteristics of synthesized polymers that could be used in the design of the biomaterial, such as: molar relationship of comonomers in the copolymer (F_i) and in the initial reaction mixture (f_i), average molecular weight (M_w), polydispersity index (PDI), reaction time (t), and percentage of reaction conversion (%C).

As can be seen in Table 1, an increment of M_w was observed when the amounts of HEMA monomers increased in the initial reaction mixture (FVH-1 vs. FVH-4). Other aspects of the different polymers were similar despite the variation in reaction times.

The copolymers were characterized by FTIR spectroscopy (Figure 1), the main signals are (cm⁻¹): 3440 (O–H), 3067 (C–H, Ar), 2983, 2940 y 2875 (C–H aliphatic), 1735 (C=O), 763 and 697 (C–H, Ar monosubstituted).

In addition, the structure and composition of comonomers were analyzed by ¹H-NMR spectrum (Figure 2) and the assignments of resonance signals are shown in Table 2.

It is known that the different monomers reactivity during copolymerization reactions produce differences between initial comonomer mixture (f_i) and monomeric composition in the copolymer (F_i) at high conversions. The relevance of determining the F_i parameter is due to the fact that the solubility, compatibility with other polymers and the physicochemical properties depend on the content of comonomers in the macromolecular chain (F_i). Thus, the copolymer compositions were estimated from ¹H-NMR spectrum, using the integral ratio of the peaks of CH from DIPF monomer, aromatic hydrogen from VBz monomer and CH₂-OH from HEMA monomer at 4.8, 8.2–7.2, and 3.7 ppm, respectively, by Equations (3–5):

$$F_F = \frac{\frac{I(\text{CH})}{2}}{\frac{I(\text{CH})}{2} + \frac{I(\text{CHAR})}{5} + \frac{I(\text{CH}_2\text{-OH})}{2}} \quad (3)$$

TABLE 1 Characteristics of synthesized polymers

Polymer	f_i^* F:V:H	F_i^{**} F:V:H	F_i^{**} F:V:H	M_w (g/mol)	PDI	t (h)	% C
FVH-1	50:37.5:12.5	47:39:14	54:42:4	6000	1.7	22	37.5
FVH-2	50:37.5:12.5	47:39:14	53:43:4	10,200	2.7	28	71.0
FVH-3	46:35:19	44:36:20	54:40:6	10,700	2.3	24	60.0
FVH-4	48:36:16	45:37:17	49:41:10	12,000	1.9	14	60.0

Note: [AIBN] = 15 mM, THF (15%v/v); *gravimetrically determined; ** Calculated from ¹H-NMR.

$$F_V = \frac{I(\text{CHAR})}{\frac{I(\text{CH})}{2} + \frac{I(\text{CHAR})}{5} + \frac{I(\text{CH}_2\text{-OH})}{2}} \quad (4)$$

$$F_H = \frac{I(\text{CH}_2\text{-OH})}{\frac{I(\text{CH})}{2} + \frac{I(\text{CHAR})}{5} + \frac{I(\text{CH}_2\text{-OH})}{2}} \quad (5)$$

where F_F , F_V , and F_H are the mole fraction of DIPF, VBz, and HEMA in the copolymer, respectively. The monomeric compositions were determined for all the synthesized copolymers (see Table 1), finding that the content of fumaric monomer in all cases is at least 50% of the molar composition of the comonomers in the copolymer. These F_i values allow obtaining polymers which are soluble in THF, acetic acid, and others.

TABLE 2 Assignments of $^1\text{H-NMR}$ spectrum of FVH-4

FVH structure	
FVH structure	
$^1\text{H-NMR}$ (Acetone- D_6) δ (ppm) assignment	8.2–7.2 (CHAR) (F); 4.8 (CH) (B); 4.1 (O- CH_2 -) (I); 3.7 (HO- CH_2 -) (J); 3.4–2.6 (O- CH - and - CH - main chain) (E,C); 2.0 (- CH_2 - main chain) (D,G); 1.2 (- CH_3) (A,H);

3.2 | Scaffolds characterization

3.2.1 | SEM analysis and macroscopic appearance

The copolymer selected to prepare membranes was FVH-4 due to its comonomers composition, high molecular weight, and acceptable conversion percentage in the shortest reaction time tested. Then the membranes were prepared by mixing the synthetic polymer with natural polymer (chitosan) and employing borax as a physic crosslinking agent, as indicated in the membrane preparation section. Different compositions of the matrix components were tested such as 1:2 (Ch/FVH) with 4 and 6% borax and 1:3 (Ch/FVH) with 4% borax. Figure 3a,b shows the macroscopic images of two faces 1:2 (Ch/FVH) membranes with 4 and 6% borax (images are representative). Under these conditions, phase separation occurred and the surfaces were clearly heterogeneous. However, the 1:3 ratios of polymers (Ch/FVH) with 4% borax (Figure 3c,d) allowed us to obtain the best membrane

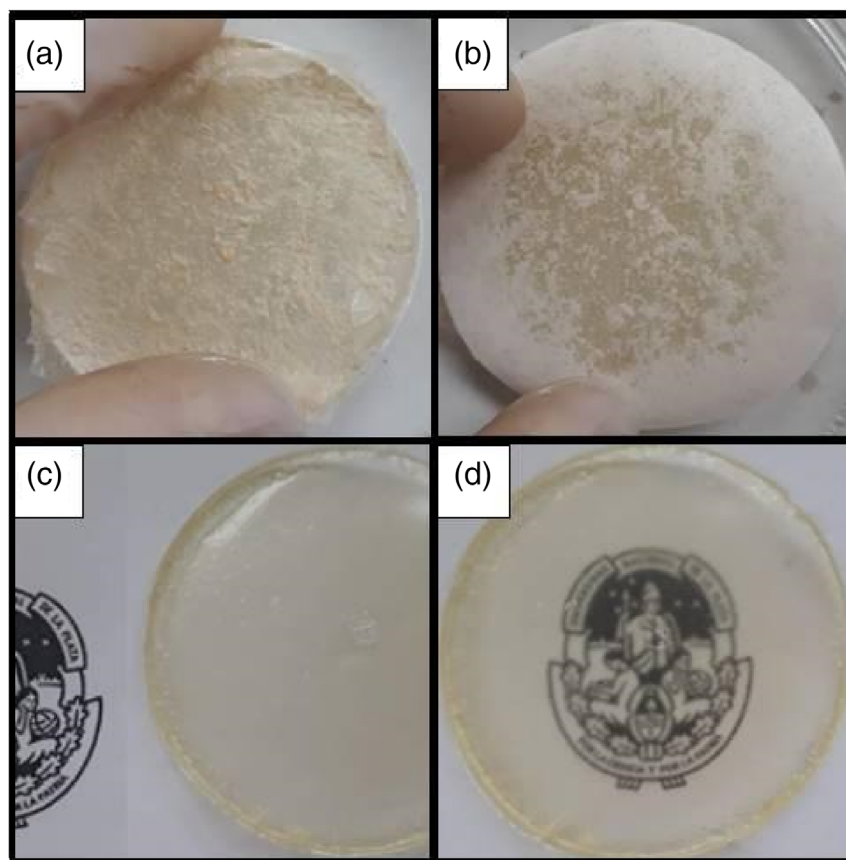


FIGURE 3 (a,b) Macroscopic aspect of 1:2 (Ch/FVH) and (c,d) 1:3 (Ch/FVH) membranes

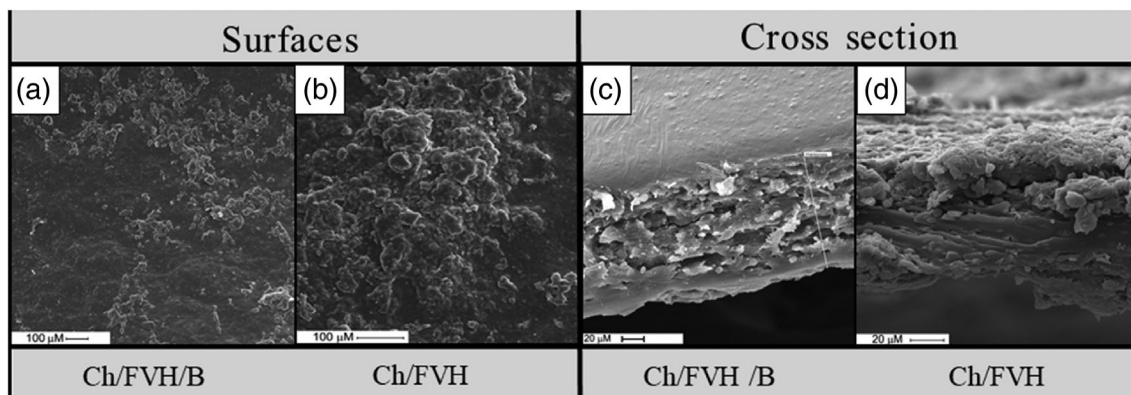


FIGURE 4 Scanning electron micrographs of Ch/FVH/B, with borax (a surface and c cross section) and Ch/FVH, without borax (b surface and d cross section)

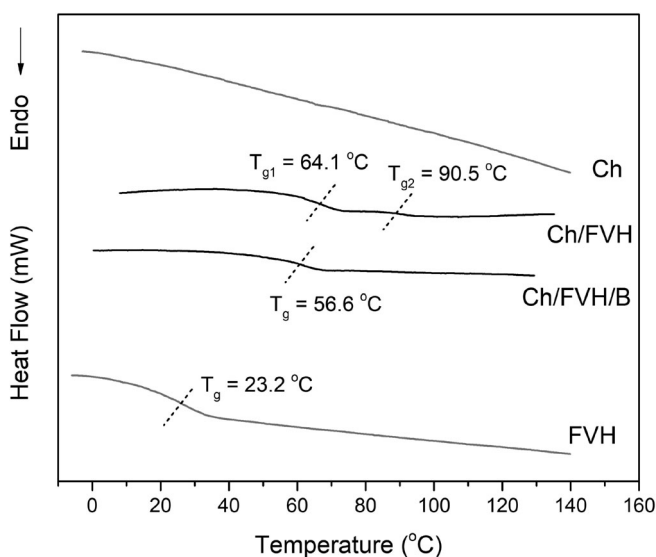


FIGURE 5 DSC thermograms of the membranes prepared from FVH, Ch/FVH/B, Ch/FVH, and Ch

in terms of its physical appearance, qualitative analysis and handling, revealing a slightly transparent surface with no apparent heterogeneity.

The average thickness of the membrane obtained under the selected conditions was also measured and the value was $114 \pm 6 \mu\text{m}$. In order to analyze the topography of the materials obtained by crosslinking with borax or physical mixing (without borax), SEM images were taken. These are shown in Figure 4.

SEM images (Figure 4a,b) of the membrane surface morphology prepared by combining FVH and chitosan (with or without borax) shows a rough, not very porous surfaces and the physical mixture presents a somewhat more heterogeneous surface than the cross-linked, respectively. Figure 4c,d presents the SEM cross section of both mentioned materials, respectively. As can be seen in Figure 4c, the membrane with borax shows no phase separation, indicating good compatibility between both polymeric components with cross-linked.

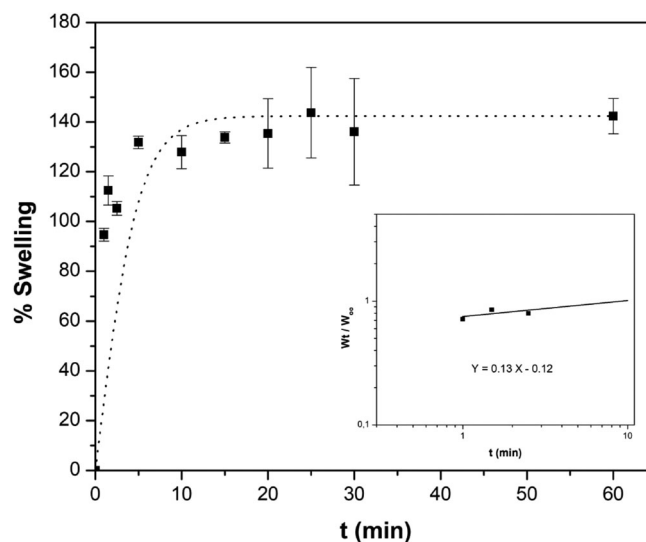


FIGURE 6 Percentage of PBS swelling of Ch/FVH/Bas a function of time at 37°C . The dot line is an eye guide

3.2.2 | Glass transition temperature evaluation

In order to verify the phase compatibility, T_g of the membranes was determined by DSC analysis. Figure 5 shows the differential scanning calorimetry analysis of Ch/FVH/B, Ch/FVH, and Ch and FVH for comparison. Is it possible to see that Ch/FVH/B exhibits only one T_g , greater than that of the FVH copolymer, while sample without borax shows two clear transitions at 64.1°C and 90.5°C , which suggests that two separated phases are present.

3.2.3 | Swelling

The swelling behavior of the membranes in an environment similar to the human body (PBS, pH 7.4 at 37°C) was analyzed. Figure 6 shows the swelling in PBS at different times of the membrane obtained with borax.

In addition, to know the kinetics of the mentioned process, the slope index n was analyzed using the Fick model (see the insert in Figure 6).

It can be seen that the degree of swelling increases with time, particularly a rapid increase in the percentage of swelling up to 5 min occurs, which reaches equilibrium close to 10 min, with a maximum value between 130% and 140%.

The diffusion of small molecules depends on the physical properties of the polymer network and the interactions between polymer segments and small molecules. According to Fick's second law, the power law equation can be used to determine the type of diffusion of water in hydrogels. The inset in Figure 6 shows the linear regression plot of the fractional-water absorbed at short times according to Equation (2), from which the n value of 0.13 ± 0.04 could be calculated indicating that the transport mechanism is controlled by Fick diffusion.

3.2.4 | Mechanical properties

The mechanical properties of Ch/FVH/B membranes were measured by traction test, after the samples were placed overnight in controlled humidity media (70%). The elastic modulus, tensile strength and

elongation at break, were 1.0 ± 0.2 MPa, 0.20 MPa ± 0.03 , and $4.8 \pm 1.5\%$, respectively.

3.3 | Biocompatibility and cytotoxicity study

3.3.1 | Biocompatibility

Since the designed materials in the present research are intended to be applied in bone or cartilaginous tissue regeneration, is important to know the cellular response to them. Thus, the cellular adhesion and proliferation of RAW 264.7 cells and BMPC seeded on the membrane were studied. Figure 7a shows the growth of RAW 264.7 macrophages evaluated by the MTT test after 2 h (adhesion) and 24 h (proliferation). In addition to completing the analysis, a similar test was carried out with BMPC during 2 h (adhesion) and 48 h (proliferation) (see Figure 7b). We found similar adhesion for both cell types on the membrane and on the tissue culture plate. Instead, after 24 h of culture, the RAW 264.7 cells proliferate better over culture plate (control) than over membranes ($p < .001$). On the other hand, no differences were found when BMPC grew on standard tissue culture

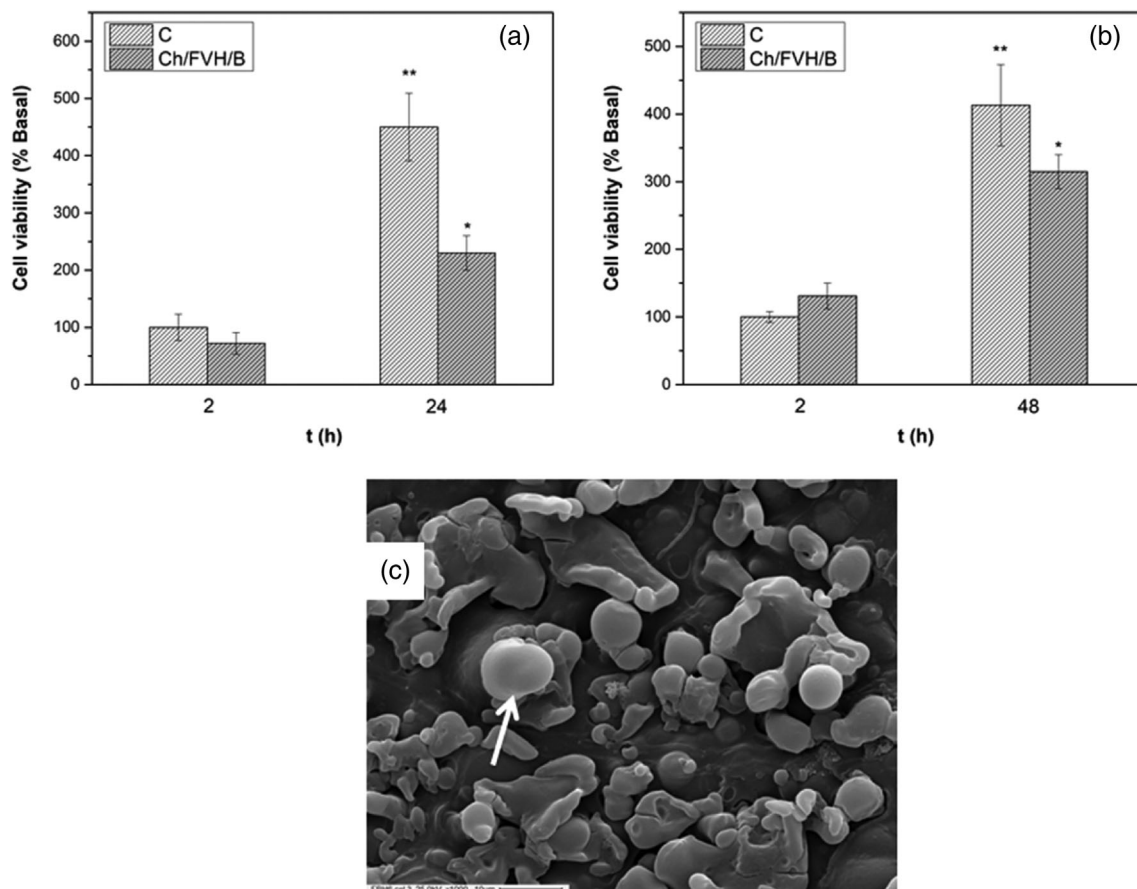


FIGURE 7 Adhesion (2 h) and proliferation (24 or 48 h) of RAW 264.7 cells (a) and BMPC (b). Panel a and b represent the survival cells evaluated by MTT assay. Results are expressed as % of Basal (cells growing on standard culture plates) and represent the mean \pm SEM, $n = 6$. Differences were: * $p < 0.01$; ** $p < 0.001$ versus basal (adhesion at 2 h on standard tissue culture plate). Panel c shows SEM image of RAW 264.7 cells (arrow indicates) growing on the surface of the membrane. Magnification $\times 1000$

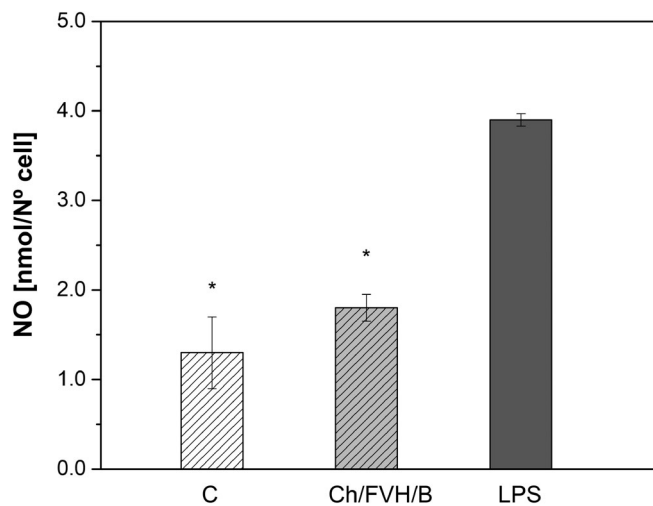


FIGURE 8 NO production determined by Griess' reaction using RAW 264.7 macrophages after 24 h of culture growing on standard tissue culture plates (C), membranes or the control plates under the presence of LPS. Results represent the mean \pm SEM, $n = 6$. Differences were: * $p < .001$ versus LPS

plate (C) or the membrane after 48 h of culture. Figure 7 also shows the morphology of RAW 264.7 cells growing on the membrane after 24 h of culture observed by SEM.

3.4 | Cytotoxicity

To evaluate the possible cytotoxicity of the membrane, NO production was assessed after 24 h of culture (Figure 8). Since macrophages have the capacity to react toward foreign bodies producing inflammation mediators such as IL, TNF α , and NO, this assay represent a good model to investigate the possible cytotoxicity of biomaterials.^{23,33,34}

4 | DISCUSSION

The copolymers employed in this study were synthesized by conventional radical polymerization, at different reaction times to achieve suitable reaction conversion without chain transfer reactions (gel fraction) and to obtain molar relationship of comonomers in the copolymer adequate to interact with chitosan and borax. Other reaction conditions (different from Table 1), such as initiator concentration [I], monomeric molar ratio in the initial reaction mixture (f_i) and reaction time were tested but gel product was obtained. Because the biomaterial will be used to prepare membranes by the solvent casting methodology, the copolymer to be used must be soluble, thus the products of the reaction as gels are not useful for this research. According to the previous studies^{35,36} the interaction between synthetic polymer, borax and natural polymer is through OH interaction, thus the samples from FVH-1 to FVH-3 are not adequate to prepare a stable membrane without phase separation (the quantity of HEMA monomer is low). Then, the sample named FVH-4 was selected to prepare the

membranes due to its high molecular weight and acceptable conversion percentage in the shortest reaction time tested. In addition, the selected copolymer was compatible with the natural polymer used in the preparation of the membrane, as it was detailed in the scaffolds preparation and characterization section. Cross-linked Ch / FVH membranes were obtained by solvent casting methodology and its physicochemical and biological properties were analyzed.

Due to the possible applications of these biomaterials in regenerative medicine, their superficial characteristics are relevant because surface chemistry and topographic characteristics (roughness, porosity and nanostructure) play an important role in cell adhesion, proliferation and differentiation.^{29,37,38} As it can be seen by scanning electron microscopy analysis, the membrane with borax shows no phase separation, indicating good compatibility between both polymeric components and the crossover agent. In order to verify this result a DSC analysis was carried out. The membrane prepared with borax addition shows a Tg value higher than FVH copolymer, which can be attributed to the restriction on the catenary movements caused by the crosslinking between both polymers with borax. On the other hand, Ch/FVH membrane exhibited two Tg values, both higher than those of FVH, which could be due to noncovalent inter- and intra-chain interactions of both polymer components. These interactions do not seem to be strong enough to favor the compatibility of the phases.

Another relevant aspect to evaluate in biomaterials is the ability of liquid uptake through capillary force, known as swelling behavior. This property is one of the more relevant features of biomaterials oriented to the application in tissue engineering, because it plays a vital role in absorption of fluids and transportation of nutrients (for example cell culture medium), oxygen, metabolites and removal of cellular waste products within membranes.³⁹ Our materials show a liquid incorporation profile similar to other systems employed in tissue engineering, which shows that it has the necessary properties mentioned above.^{40,41}

As it was mentioned before, tissue engineering is a field in which functional substitutes (scaffolds) for damaged tissues and organs are developed. The scaffold serves as a mechanical substrate for cells and bioactive factors and can help direct and organize the process of regeneration of different tissues. Each one of those tissues has different and particular mechanical properties, depending on its function.^{42,43} For instance, mechanical properties of cartilage allow the movement of liquid component during loading, across the tissue. Their mechanical properties depend on the stiffness and strength of the collagen network and should be considered in designing a scaffold.⁴⁴ Due to values obtained of elastic modulus, tensile strength and elongation at break, our results are comparable to the mechanical properties of other structural related systems.^{23,35} Lu et al. has described a Young' Modulus value for native cartilage is between 0.32 and 1.02 MPa,⁴⁵ while in a recent review⁴⁴ it was reported values between 0.4 and 0.8 MPa. Thus, the mechanical characteristics of the biomaterial developed in the present study suggest that this material could be suitable for medical application in the treatments of cartilage disorders. However, more extensive in vitro and in vivo studies would be necessary in order to test the specific applications of this material.

The biocompatibility and cytotoxicity of membranes were analyzed in order to investigate the in vitro behavior of the designed materials. From SEM images it was possible to see that the cell's morphology showed a round aspect, indicating good cell interaction with the matrix, maintaining the typical morphology of RAW cells, as previously reported.^{29,46} Therefore, these results suggest that the membrane presents a good biocompatibility with cell line tested. Analogous results were found in the BMPC growth with similar scaffolds.²³ Moreover, we found that NO production was similar when cells had been grown on control wells or on the membrane. In addition, when the cells growing on standard tissue culture plates were exposed to lipopolysaccharide (LPS) as a positive control of cytotoxicity, cells respond to the toxic agent increasing the NO production into the conditioned media after 24 h of culture. These results suggest that the membrane did not generate any toxicity under the conditions studied.

5 | CONCLUSIONS

In this study, the synthesis conditions of a new terpolymer were optimized and a copolymer with expected characteristics to combine with natural polymer was obtained. In addition, it was possible to design a homogeneous membrane from borax cross-linked fumaric terpolymer and chitosan. This membrane exhibited adequate surface morphology, swelling capacity and good mechanical properties for regenerative medicine. Furthermore, this material shows a good biocompatibility without evidence of cytotoxicity. Altogether the results suggest that the designed material could be applied in scaffolds for osteochondral engineering.

ACKNOWLEDGMENTS

This study was partially supported by grants from Facultad de Ciencias Exactas, Universidad Nacional de La Plata (UNLP, 11/X769), CONICET (PIP D0047). M. Leticia Bravi Costantino is a fellowship of Conicet; M. Soledad Belluzo, Tamara G. Oberti, and M. Susana Cortizo are members of Carrera del Investigador Científico of CONICET and Ana M. Cortizo is member of Carrera del Investigador Científico of CICPBA.

DATA AVAILABILITY STATEMENT

The data that support the findings of this study are available from the corresponding author upon reasonable request.

ORCID

Tamara G. Oberti  <https://orcid.org/0000-0001-8641-747X>

REFERENCES

- Biswal T, Badjena SK, Pradhan D. Sustainable biomaterials and their applications: a short review. *Mater Today*. 2020;30:274-282.
- Turnbull G, Clarke J, Picard F, et al. 3D bioactive composite scaffolds for bone tissue engineering. *Bioact Mater*. 2018;3:278-314.
- Khare D, Basu B, Dubey AK. Electrical stimulation and piezoelectric biomaterials for bone tissue engineering applications. *Biomaterials*. 2020;258:120280-120280.
- MacNeil S. Biomaterials for tissue engineering of skin. *Mater Today*. 2008;11:26-35.
- Armiento AR, Stoddart MJ, Alini M, Eglin D. Biomaterials for articular cartilage tissue engineering: Learning from biology. *Acta Biomater*. 2018;65:1-20.
- Torres ML, Oberti TG, Fernández JM. HEMA and alginate-based chondrogenic semi-interpenetrated hydrogels: synthesis and biological characterization. *J Biomater Sci Polym Ed*. 2020;1-15. <https://doi.org/10.1080/09205063.2020.1849920>
- Sultankulov B, Berillo D, Sultankulova K, Tokay TL, Saparov A. Progress in the development of chitosan-based biomaterials for tissue engineering and regenerative medicine. *Biomolecules*. 2019;9:470.
- Janoušková O. Synthetic polymer scaffolds for soft tissue engineering. *Physiol Res*. 2018;67:S335-S348.
- Otsu T, Matsumoto A, Shiraishi K, Amaya N, Koinuma Y. Effect of the substituents on radical copolymerization of dialkyl fumarates with some vinyl monomers. *J. Polym. Sci., Part A Polym. Chem*. 1992;30:1559-1565.
- Al-Arbash AH, Elsaygher FA, Ali AAM, Elsaygher MZ. Glass-transition temperature of polydialkyl fumarate copolymers. *J Polym Sci Part A: Polym Chem*. 1999;37:1839-1845.
- Fernandez JM, Molinuevo MS, Cortizo AM, McCarthy AD, Cortizo MS. Characterization of poly (ϵ -caprolactone)/polyfumarate blends as scaffolds for bone tissue engineering. *J Biomat Sci Pol Ed*. 2010;21:1297-1312.
- Pasqualone M, Oberti TG, Andreetta HA, Cortizo MS. Fumarate copolymers-based membranes overlooking future transdermal delivery devices: synthesis and properties. *J Mater Sci Mater Med*. 2013;24:1683-1692.
- Belluzo MS, Medina LF, Cortizo AM, Cortizo MS. Ultrasonic compatibilization of polyelectrolyte complex based on polysaccharides for biomedical applications. *Ultrason Sonochem*. 2016;30:1-8.
- Lastra ML, Molinuevo MS, Blaszczyk-Lezak I, Mijangos C, Cortizo MS. Nanostructured fumarate copolymer-chitosan crosslinked scaffold: an in vitro osteochondrogenesis regeneration study. *J Biomed Mater Res A*. 2018;106:570-579.
- Kurita K. Chitin and chitosan: functional biopolymers from marine crustaceans. *Mar Biotechnol*. 2006;8:203-226.
- Rinaudo M. Chitin and chitosan: properties and applications. *Prog Polym Sci*. 2006;31:603-632.
- Croisier F, Jérôme C. Chitosan-based biomaterials for tissue engineering. *Eur Polym J*. 2013;49:780-792.
- Kim IY, Seo SJ, Moon HS, et al. Chitosan and its derivatives for tissue engineering applications. *Biotechnol Adv*. 2008;26:1-21.
- Bi S, Wang P, Hu S, et al. Construction of physical-crosslink chitosan/PVA double-network hydrogel with surface mineralization for bone repair. *Carbohydr Polym*. 2019;224:115176.
- Cui Z, Lin L, Si J, et al. Fabrication and characterization of chitosan/OGP coated porous poly(ϵ -caprolactone) scaffold for bone tissue engineering. *J Biomater Sci Polym Ed*. 2017;28:826-845.
- Aguilar A, Zein N, Harmouch E, et al. Application of chitosan in bone and dental engineering. *Molecules*. 2019;24:3009.
- Oberti TG, Cortizo MS, Alessandrini JL. Novel copolymer of diisopropyl fumarate and benzyl acrylate synthesized under microwave energy and quasielastic light scattering measurements. *J Macromol Sci Pure Appl Chem*. 2010;47:725-731.
- Lastra ML, Molinuevo MS, Cortizo AM, Cortizo MS. Fumarate copolymer-chitosan cross-linked scaffold directed to osteochondrogenic tissue engineering. *Macromol Biosci*. 2017;17:1600219.
- Cortizo MS, Laurella S, Alessandrini JL. Microwave-assisted radical polymerization of dialkyl fumarates. *Radiat Phys Chem*. 2007;76:1140-1146.
- Ritger PL, Peppas NA. A simple equation for description of solute release I. Fickian and non-fickian release from non-swellable devices

- in the form of slabs, spheres, cylinders or discs. *J Control Release*. 1987;5:23-36.
26. Brazel CS, Peppas NA. Modeling of drug release from swellable polymers. *Eur J Pharm Biopharm*. 2000;49:47-58.
 27. Ganji F, Vasheghani FS, Vashenghani FE. Theoretical description of hydrogel swelling: a review. *Iran Polym J*. 2010;5:375-398.
 28. Fernandez JM, Molinuevo MS, Cortizo MS, Cortizo AM. Development of an osteoconductive PCL-PDIPF-hydroxyapatite composite scaffold for bone tissue engineering. *J Tissue Eng Regen Med*. 2011;5:e126-e135.
 29. Bravi Costantino ML, Oberti TG, Cortizo AM, Cortizo MS. Matrices based on lineal and star fumarate-metha/acrylate copolymers for bone tissue engineering: characterization and biocompatibility studies. *J Biomater Res A*. 2019;107:195-203.
 30. Bravi Costantino ML, Cortizo MS, Cortizo AM, Oberti TG. Osteogenic scaffolds based on fumaric/N-isopropylacrylamide copolymers: Designed, properties and biocompatibility studies. *Eur Polym J*. 2020;122:109348.
 31. Committee for the Update of the Guide for the Care and Use of Laboratory Animals. UFA P, ed. Guidelines on handling and training of laboratory animals. *The biological council of animal research, welfare panel. Guide for the care and use of laboratory animals*. 8th ed. Washington D.C: The National Academies Press; 2011.
 32. Fernández JM, Cortizo MS, Cortizo AM. Fumarate/ceramic composite based scaffolds for tissue engineering: evaluation of hydrophilicity, degradability, toxicity and biocompatibility. *J Biomat Tissue Eng*. 2014;4:227-234.
 33. Bixby J, Ray TD, Chan FK. TNF, cell death and inflammation. *Curr Med Chem Antiinflamm AntiAllergy Agents*. 2005;4:557-567.
 34. Denlinger LC, Fiset PL, Garis KA, et al. Regulation of inducible nitric oxide synthase expression by macrophage purinoreceptors and calcium. *J Biol Chem*. 1996;271:337-342.
 35. Liang S, Liu L, Huang Q, Yam KL. Preparation of single or double-network chitosan/poly (vinyl alcohol) gel films through selectively cross-linking method. *Carbohyd Polym*. 2009;77:718-724.
 36. Keita G, Ricard A, Audebert R, Pezron E, Leibler L. The poly(vinyl alcohol)-borate system: Influence of polyelectrolyte effects on phase diagrams. *Polymer*. 1995;36:49-54.
 37. Lastra ML, Molinuevo MS, Giussi JM, et al. Tautomerizable β -ketonitrile copolymers for bone tissue engineering: studies of biocompatibility and cytotoxicity. *Mater Sci Eng C*. 2015;51:256-262.
 38. Coppari S, Ramakrishna S, Teodori L, Albertini MC. Cell signalling and biomaterials have a symbiotic relationship as demonstrated by a bioinformatics study: the role of surface topography. *Curr Opin Biomed Eng*. 2020;17:100246.
 39. Lee HJ, Ahn SH, Kim GH. Three-dimensional collagen/alginate hybrid scaffolds functionalized with a drug delivery system (DDS) for bone tissue regeneration. *Chem Mater*. 2012;24:881-891.
 40. Belluzo MS, Medina LF, Molinuevo MS, Cortizo MS, Cortizo AM. Nanobiocomposite based on natural polyelectrolytes for bone regeneration. *J Biomed Mater Res*. 2020;108:1467-1478.
 41. Govindharaj M, Roopavath UK, Rath SN. Valorization of discarded Marine Eel fish skin for collagen extraction as a 3D printable blue biomaterial for tissue engineering. *J Clean Prod*. 2019;230:412-419.
 42. Kelly TAN, Roach BL, Weidner ZD, et al. Tissue-engineered articular cartilage exhibits tension compression nonlinearity reminiscent of the native cartilage. *J Biomech*. 2013;46:1784-1791.
 43. Gurumurthy B, Janorkar AV. Improvements in mechanical properties of collagen-based scaffolds for tissue engineering. *Curr Opin Biomed Eng*. 2020;17:100253.
 44. Cipollaro L, Ciardulli MC, Della Porta G, Peretti GM, Maffulli N. Biomechanical issues of tissue-engineered constructs for articular cartilage regeneration: in vitro and in vivo approaches. *Br Med Bull*. 2019;132(1):53-80.
 45. Lu L, Zhu X, Valenzuela RG, Currier BL, Yaszemski MJ. Biodegradable polymer scaffolds for cartilage tissue engineering. *Clin Orthop Relat Res*. 2001;391:S251-S270.
 46. Fernandez JM, Oberti TG, Vikingsson L, Ribelles JLG, Cortizo AM. Biodegradable polyester networks including hydrophilic groups favor BMSCs differentiation and can be eroded by macrophage action. *Polym Degrad Stab*. 2016;130:38-46.

How to cite this article: Bravi Costantino, M. L., Belluzo, M. S., Oberti, T. G., Cortizo, A. M., & Cortizo, M. S. (2022). Terpolymer-chitosan membranes as biomaterial. *Journal of Biomedical Materials Research Part A*, 110(2), 383–393. <https://doi.org/10.1002/jbm.a.37295>